

IMPROVED DYNAMIC PERFORMANCE OF DIRECT TORQUE CONTROL OF
INDUCTION MACHINES

AUZANI BIN JIDIN

UNIVERSITI TEKNOLOGI MALAYSIA

IMPROVED DYNAMIC PERFORMANCE OF DIRECT TORQUE CONTROL OF
INDUCTION MACHINES

AUZANI BIN JIDIN

A thesis submitted in fulfilment of the
requirements for the award of the degree of
Doctor of Philosophy (Electrical Engineering)

Faculty of Electrical Engineering
Universiti Teknologi Malaysia

MAY 2011

*To my beloved wife, son, daughters and all my family members
for their enduring love, motivation and support*

ACKNOWLEDGEMENT

I would like to express my deep gratitude to my supervisor Associate Prof. Dr. Nik Rumzi Bin Nik Idris for his invaluable suggestions, guidance and consistent support towards the completion of this thesis. Special thank to my co supervisors Prof. Ir. Dr. Halim Mohd. Yatim and Prof. Malik Elbuluk for valuable guidance and generous encouragement throughout the project duration.

I would like to thank the many people who have contributed to this thesis. In particular, to the members of academic and technical staff of the Energy Conversion Department (ENCON), Universiti Teknologi Malaysia for the cooperation and technical help.

I also wish to express my gratitude to the Universiti Teknikal Malaysia Melaka (UTeM) and the Ministry of Higher Education for providing the sponsorship to undertake this study.

Finally, I would like to thank my parents, my wife Nurul Adibah, my son Amirul Haziq, my daughters 'Alya Insyirah and Aisyah Humaira for their loves, encouragement and moral support.

ABSTRACT

This thesis proposes simple methods to improve the dynamic performances of a Direct Torque Control (DTC) of induction machines. The principles of direct control of torque and flux based on the selection of appropriate voltage vectors are reviewed. In DTC, the torque is directly controlled by the slip angular frequency which is determined by the irregular motion of stator flux vector. The stator flux is always forced to follow its circular reference by the application of active voltage vectors. During a large torque demand, no zero voltage vector is used. However, the active voltages are switched more often to increase (or decrease) rapidly the slip and the output torque as well. Moreover, this method does not give the fastest dynamic torque response because one of the two possible active voltage vectors switched during torque dynamic is not optimal. The effect of selecting two different voltages on torque dynamic response is investigated and evaluated. Based on the investigation, the most optimized voltage is identified, and it is used to perform a dynamic overmodulation to produce the fastest torque dynamic control. The improved torque dynamic control is verified by simulation and experimental results. Owing to the intrinsic characteristic of DTC switching, it is not possible for stator voltage to perform a six-step mode. The thesis proposes a simple overmodulation strategy for hysteresis-based DTC by transforming the flux locus into a hexagonal shape. This is accomplished by modifying the flux error status before it is being fed to a look-up table. In this way, a smooth transition of stator voltage from Pulse Width Modulation to the six-step mode is achieved as the number of application of zero voltage vectors, i.e. during the motor acceleration, is gradually dropped to zero. With the six-step voltage operation, it allows the DTC to extend a constant torque region and hence results in higher torque capability in a field weakening region. To verify the improvement of the proposed method, simulation and experimentation as well as comparison with the conventional DTC scheme are carried out. It can be shown that the improvement about 20% (in terms of extension of constant torque region) can be achieved through the proposed method. The improvements mentioned above can also be achieved in the DTC with constant frequency torque controller that offers constant switching frequency and reduced torque ripple. The improvements are verified by experimental results.

ABSTRAK

Tesis ini mencadangkan kaedah mudah untuk meningkatkan prestasi dinamik bagi sebuah Kawalan Dayakilas Terus (DTC) untuk mesin aruhan. Prinsip kawalan terus dayakilas dan fluks berpandukan pemilihan vektor voltan yang sesuai, diulangkaji. Dalam DTC, dayakilas dikawal secara langsung oleh frekuensi sudut gelincir yang ditentukan oleh pergerakan tidak teratur oleh vektor fluks pemegun. Fluks pemegun sentiasa dipaksa untuk mengikut rujukan membulat dengan aplikasi vektor voltan aktif. Semasa permintaan daya kilas yang besar, tiada vektor voltan sifar digunakan. Tetapi, pensuisan voltan-voltan aktif lebih kerap untuk meningkatkan (atau mengurangkan) dengan pantas gelinciran dan juga keluaran dayakilas. Tambahan lagi, kaedah ini tidak memberikan sambutan dayakilas dinamik yang terpanas kerana salah satu daripada dua kemungkinan voltan aktif yang dipilih semasa dinamik dayakilas adalah tidak optimum. Kesan bagi pemilihan dua voltan yang berbeza terhadap sambutan dayakilas dinamik, diselidik dan dinilai. Berdasarkan penyelidikan ini, voltan yang paling optimum dikenalpasti, dan digunakan untuk operasi dinamik permodulatan lebih bagi menghasilkan kawalan dayakilas dinamik terpanas. Peningkatan kawalan dayakilas dinamik ini disahkan oleh keputusan simulasi dan eksperimen. Disebabkan ciri-ciri semulajadi pensuisan DTC, ianya tidak memungkinkan untuk voltan pemegun untuk beroperasi pada mod enam langkah. Tesis ini mencadangkan strategi permodulatan lebih yang ringkas bagi DTC berasaskan histeresis dengan mengawal lokus fluks kepada bentuk heksagon. Ini dapat dilakukan dengan mengubahsuai status kesalahan fluks sebelum dimasukkan ke dalam jadual pemilihan. Melalui cara ini, kelancaran peralihan voltan pemegun dari Pemodulatan Lebar Denyut ke mod enam langkah dicapai apabila jumlah aplikasi vektor voltan sifar, iaitu semasa pecutan motor, diturunkan secara perlahan-lahan kepada sifar. Dengan operasi voltan enam langkah, ia membolehkan DTC memperluaskan kawasan dayakilas tetap dan seterusnya menghasilkan keupayaan dayakilas yang lebih tinggi di dalam kawasan pelemahan medan. Untuk mengesahkan penambahbaikan oleh cadangan kaedah, simulasi dan eksperimen serta perbandingan dengan skim konvensional DTC dijalankan. Dapat ditunjukkan bahawa penambahbaikan sekitar 20% (dalam hal memperluaskan kawasan dayakilas tetap) boleh dicapai melalui kaedah yang dicadangkan. Penambahbaikan yang disebut di atas juga boleh dicapai dalam DTC dengan pengawal dayakilas frekuensi tetap yang menawarkan frekuensi pensuisan malar dan pengurangan riak dayakilas. Penambahbaikan ini disahkan oleh keputusan eksperimen.

TABLE OF CONTENTS

CHAPTER	TITLE	PAGE
	DECLARATION	ii
	DEDICATION	iii
	ACKNOWLEDGEMENTS	iv
	ABSTRACT	v
	ABSTRAK	vi
	TABLE OF CONTENTS	vii
	LIST OF TABLES	xii
	LIST OF FIGURES	xiii
	LIST OF SYMBOLS AND ABBREVIATIONS	xxiii
	LIST OF APPENDICES	xxvi
1	INTRODUCTION	1
	1.1 A Look Back on Development of Vector Control Induction Machine Drives	1
	1.2 Direct Torque Control of Induction Machines	2
	1.2.1 The Control Structure of Basic DTC	2
	1.2.2 Improvements of DTC Performance	4
	1.2.3 The Popularity Versus The Complexity of DTC-SVM based induction machines	9
	1.3 Thesis Objectives and Contributions	10
	1.4 Methodology of Research	12
	1.5 Organisation of the Thesis	14

2	OVERVIEW OF CONVENTIONAL DIRECT TORQUE CONTROL OF INDUCTION MACHINES	16
2.1	Introduction	16
2.2	Mathematical Model of Induction Machine	16
2.2.1	Complex Space Vector Equations	18
2.2.2	d-q Axis Equations	20
2.3	Basic Principles of Direct Torque Control	22
2.3.1	3-Phase Voltage Source Inverter Space Vectors	22
2.3.2	Direct Flux Control	24
2.3.3	Direct Torque Control	28
2.3.4	De-coupled Control of Torque and Flux in DTC-hysteresis based Induction Machine	34
2.3.5	Estimations of stator flux and electromagnetic torque	35
2.4	Major Problems in Hysteresis-Based DTC	37
2.4.1	Variable inverter switching frequency	37
2.4.2	High Torque Ripple	38
2.4.3	The Need of High Speed Processor	39
2.5	Chapter Conclusions	42
3	ENLARGING SWITCHING FREQUENCY TO MINIMIZE TORQUE RIPPLE UTILIZING A CONSTANT FREQUENCY TORQUE CONTROLLER	43
3.1	Introduction	43
3.2	DTC with Constant Frequency Torque Controller	44
3.3	Design Procedure of Constant Frequency Torque Controller in DTC	46
3.4	Experimental Set-up	49
3.5	Experimental Results	52
3.6	Chapter Conclusions	57

4	AN OPTIMIZED SWITCHING STRATEGY FOR QUICK TORQUE DYNAMIC CONTROL	58
4.1	Introduction	58
4.2	Dynamic Torque Control in the Hysteresis-Based DTC	59
4.3	Effect of Selecting Different Voltage Vectors on Torque Dynamic Performance in the Hysteresis-Based DTC	59
4.4	The Proposed Torque Dynamic Control	63
4.4.1	An Optimized Voltage Vector for Quick Torque Dynamic Control	63
4.4.2	The Proposed Control Structure	66
4.5	Simulation and Experimental Results	68
4.5.1	Simulation of the Proposed Torque Dynamic Control	69
4.5.2	Experimental Set-up	73
4.5.3	Improved Torque Dynamic Control for Hysteresis-based DTC	74
4.5.4	Improved Torque Dynamic Control for Constant Switching Frequency-based DTC	80
4.5.5	Behavior of Motor Currents during Torque Dynamic Condition	83
4.6	Chapter Conclusions	85
5	A WIDE-SPEED HIGH TORQUE CAPABILITY UTILIZING OVERMODULATION STRATEGY FOR DIRECT TORQUE CONTROL OF INDUCTION MACHINES	86
5.1	Introduction	86
5.2	Torque Capability in DTC	87
5.3	Improved Torque Capability with the Proposed Overmodulation Strategy	90
5.3.1	Extending the Stator Voltage Operation to	90

	Six-Step Mode	
5.3.2	Extending the Limit of Stator Flux Angular Frequency	93
5.3.3	Flux Weakening with Six-Step Mode	93
5.4	The Proposed Hybrid DTC Scheme	95
5.4.1	Hexagonal Flux Control in the Proposed Hybrid Scheme	96
5.4.2	Definition of Dynamic Condition	102
5.5	Simulation and Experimental Results	104
5.5.1	Simulation of the Proposed Overmodulation and Flux Weakening Strategy in the Hybrid DTC Scheme	104
5.5.2	Experimental Set-up Improved Torque Capability for Constant Switching Frequency-based DTC	110
5.5.3	Improved Torque Capability for Hysteresis-based DTC	112
5.5.4	Improved Torque Capability for Constant Switching Frequency-based DTC	117
5.6	Chapter Conclusions	121
6	DESCRIPTION OF THE EXPERIMENTAL SET-UP	122
6.1	Introduction	122
6.2	DS1102 Controller Board	124
6.3	Altera Field Programmable Gate Array – APEX20KE	129
6.4	Gate Drivers and 3-Phase Voltage Source Inverter (VSI)	132
6.5	Induction Machines	135
6.6	Chapter Conclusions	137
7	CONCLUSION AND FUTURE WORK	138
7.1	Conclusions	138
7.2	Future Work	139

REFERENCES

142

Appendices A-G

151-187

LIST OF TABLES

TABLE NO.	TITLE	PAGE
2.1	Voltage vectors selection table as proposed in [13]	35
3.1	Induction machine parameters	51
3.2	PI controllers gains and crossover frequency	52
4.1	DTC-Hysteresis based system and induction machine parameters	73
5.1	DTC-Hysteresis Based/Hybrid Systems and Induction Machine Parameters	111
6.1	Induction machine parameters	136

LIST OF FIGURES

FIGURE NO.	TITLE	PAGE
1.1	Control structure of basic DTC-hysteresis based induction machine	4
1.2	Variations of modified reference voltage vectors which is applied during dynamic overmodulation mode	7
1.3	A general block diagram of generation of switching in DTC-SVM	10
2.1	Cross-section of a single pole-pair three-phase machine	17
2.2	A space vector x in the three-phase symmetric system (based on (2.1))	19
2.3	Schematic diagram of Voltage Source Inverter (VSI)	23
2.4	Voltage space vectors of a 3-phase inverter with the corresponded switching states	24
2.5	Control of flux magnitude using a 2-level hysteresis comparator	25
2.6	Typical waveforms of the stator flux, the flux error	26

	and the flux error status for the two-level hysteresis flux comparator	
2.7	Definition of six sectors of the stator flux plane	27
2.8	Two possible active voltages are switched for each sector to control the stator flux within its hysteresis band	27
2.9	The variation of δ_{sr} with application of (a) active voltage vector, (b) zero or radial voltage vector, (c) reverse voltage vector	29
2.10	The application of voltage vectors in controlling the δ_{sr} as well as the output torque for 4-quadrant operation	31
2.11	Control of torque using a 3-level hysteresis comparator	33
2.12	Typical waveforms of the torque, the torque error and the torque error status for the three-level hysteresis torque comparator	33
2.13	A de-coupled control structure of DTC-hysteresis based induction machine	34
2.14	The waveforms of output torque sampled at DT in the hysteresis comparator for (a) low speed, (b) middle speed and (c) high speed	39
2.15	Experimental results of control of output torque utilizing three-level hysteresis comparator (in hysteresis based-DTC). (a) Hysteresis band = $2HB_{Te}$, sampling time = $2DT$, (b) hysteresis band = HB_{Te} ,	41

sampling time=2DT and (c) Hysteresis band = HB_{Te} ,
sampling time=DT

3.1	Constant frequency torque controller (CFTC)	45
3.2	Typical waveforms of the constant frequency torque controller	45
3.3	Generated upper triangular waveform using DSP (sampled at $DT \mu s$)	46
3.4	Averaged and linearized torque loop (as proposed in [32])	49
3.5	Generated upper triangular waveforms sampled at $55 \mu s$. (a) <i>DTC-CSF1</i> , (b) <i>DTC-CSF2</i> and (c) <i>DTC-CSF3</i>	51
3.6	Bode plot of loop gain with PI controller for (a) <i>DTC-CSF1</i> , (b) <i>DTC-CSF2</i> and (c) <i>DTC-CSF3</i>	52
3.7	Experimental results of phase current frequency spectrum and output torque for the basic DTC, <i>DTC-CSF1</i> , <i>DTC-CSF2</i> and <i>DTC-CSF3</i> at the speed about (a) 20 rad/s (b) 30 rad/s and (c) 55 rad/s	54
3.8	Experimental results for step response of torque in (a) DTC-hysteresis based, (b) <i>DTC-CSF1</i> , (c) <i>DTC-CSF2</i> and (d) <i>DTC-CSF3</i> . (1) is output torque, (2) is reference torque, (3) is torque error, (4) is output of PI controller, (5) is upper triangular waveform, (6) is torque error status. (x-axis or time scale: 2 ms/div.)	55

3.9	The zoomed image (zoomed area indicated by '↔') of the waveforms of upper triangular and output of PI controller for (a) <i>DTC-CSF1</i> , (b) <i>DTC-CSF2</i> and (c) <i>DTC-CSF3</i> , corresponds the results obtained in Figure 3.8 (b),(c) and (d). (Time scale: 1 ms/div.)	56
3.10	Experimental results of output torque, motor speed and d-axis flux component for a square-wave speed reference for (a) the basic DTC and (b) <i>DTC-CSF2</i> based induction machine drives	57
4.1	The selection of two possible active voltage vectors in controlling the flux in Sector III	60
4.2	Space vectors of the applied voltage, the stator flux and the rotor flux	61
4.3	Inconsistent torque slope due to selection of different voltage vectors	62
4.4	Effects of selecting different switching modes under torque dynamic conditions (a) when the stator flux is about to enter sector h, (b) when the stator flux is at the middle of sector h	64
4.5	Comparison of the load angle, $\Delta\delta_{sf}$ for three different modes of switching under torque dynamic conditions (a) when the stator flux is about to enter sector h (b) when the stator flux is at the middle of sector h	65
4.6	Structure of DTC-hysteresis based induction machine with the proposed modification of flux error status	67

4.7	The proposed digital outputs in modified flux error status correspond to the optimized voltage vectors for every subsector in each sector	68
4.8	Simulink blocks of the DTC drive with the proposed block of modification of flux error status	70
4.9	Identification of flux sector and determination of the appropriate flux error status in the block of modification of flux error status	71
4.10	Generation of reference torque from 1.5 Nm to 9 Nm at a specific flux positions (i.e. case1 at the middle Sector II or case2 at the boundary Sector I and II)	72
4.11	Experimental Set-up (DTC with torque control loop)	74
4.12	Comparison by simulation and experimental of dynamic torque performance between (a) <i>DTC1</i> and (b) <i>DTC2</i> , when a dynamic torque control occurs as the stator flux position at $\alpha_h = \pi/24$ rad.	76
4.13	Comparison by simulation and experimental of dynamic torque performance between (a) <i>DTC1</i> and (b) <i>DTC2</i> , when a dynamic torque control occurs as the stator flux position at $\alpha_h = \pi/6$ rad. (at the middle of Sector II)	77
4.14	Comparison of stator flux locus obtained in (a) <i>DTC1</i> and (b) <i>DTC2</i> (for one complete flux wave cycle) when a dynamic torque condition occurs at $\alpha_h = \pi/24$ rad.	78

4.15	Comparison of stator flux locus obtained in (a) <i>DTCI</i> and (b) <i>DTC2</i> (for one complete flux wave cycle) when a dynamic torque condition occurs at $\alpha_h=\pi/6$ rad.	79
4.16	Structure of DTC-constant switching frequency (DTC-CSF) based induction machine with the proposed modification of flux error status block	80
4.17	Comparison by experimental of dynamic torque performance for (a) <i>DTCI</i> , (b) <i>DTC2</i> and (c) <i>DTC-CSF2</i> when a dynamic torque control occurs as the stator flux position at $\alpha_h=\pi/24$ rad.. (1) is stator flux (Wb), (2) is flux error status, (3) is output torque (Nm) and (4) is torque error status	81
4.18	Comparison by experimental of dynamic torque performance for (a) <i>DTCI</i> , (b) <i>DTC2</i> and (c) <i>DTC-CSF2</i> when a dynamic torque control occurs as the stator flux position at $\alpha_h=\pi/6$ rad.. (1) is stator flux (Wb), (2) is flux error status, (3) is output torque (Nm) and (4) is torque error status	82
4.19	The behavior of motor currents since the flux magnitude suddenly distorted due to the proposed switching strategy as the dynamic torque occurs at $\alpha_h=\pi/24$ rad. and $\alpha_h=\pi/6$ rad. The dynamic torque control is applied at three different speed operations for (a) at around 100 rpm (b) at around 300 rpm (c) at around 540 rpm	84
5.1	Phasor diagrams of vectors of stator voltage, ohmic voltage drop and back-emf for (a) low speed operation and (b) base speed operation	88

5.2	The mapping of the voltage vector and the stator flux trajectories	92
5.3	The comparison of the performances of stator voltage and torque capability for (a) DTC without the proposed overmodulation and (b) DTC with the proposed overmodulation (Time scale: 162.5 ms/div.)	92
5.4	More rapid motor acceleration achieved with the proposed overmodulation and flux weakening strategy when a step change of reference speed is applied at time t_1	95
5.5	The structure of hybrid DTC of induction motor drive with the proposed block of ‘modification of flux error status’	97
5.6	Ideal case of hexagonal flux control based on Ψ_s^-	98
5.7	Effect of ohmic voltage drop on the trajectory of stator flux vector. (a) stator flux locus (b) phasor diagram of (5.3)	100
5.8	Flux keeps the increase as it enters to subsector ii until it reaches to the point c . (i.e. path $b-c$) with the $\Psi_{s,mod}^- = 0$	101
5.9	State diagram of finite state machine that establishes the modified flux error status ($\Psi_{s,mod}^-$) for proper hexagonal flux locus operation	101
5.10	The selection of flux error status in the block of modification of flux error status. (a) Original flux	103

	error status Ψ_s^+ for circular locus (b) Modified flux error status $\Psi_{s,mod}^-$ for hexagonal locus	
5.11	Block diagram of a PI speed controller and flux weakening algorithm	103
5.12	Simulink blocks of the DTC drive with the proposed block of modification of flux error status and the block of a PI speed controller and a flux weakening algorithm	107
5.13	Identification of flux sector and determination of the appropriate flux error status $\Psi_{s,mod}^-$ (based on Figure 5.9), in the block of modification of flux error status	108
5.14	Generation of references of torque and stator flux from a PI speed controller and flux weakening algorithm	109
5.15	Experimental Set-up (DTC with speed control loop)	110
5.16	Comparison of capability of torque obtained in (a) <i>DTC-HYS1</i> and (b) <i>DTC-HYS3</i> (Time scale: 400ms/div.)	113
5.17	Comparison of torque control as the speed reaches its target for (a) <i>DTC-HYS2</i> and (b) <i>DTC-HYS3</i> (Time scale: 400ms/div.)	115
5.18	Stator flux locus correspond to the results obtained in Figures 5.16 and 5.17 for (a) <i>DTC-HYS1</i> , (b) <i>DTC-HYS2</i> and (c) <i>DTC-HYS3</i>	116

5.19	Comparison performances of torque capability, current wave shape and torque ripple in (a) <i>DTC-HYS1</i> , (b) <i>DTC-HYS3</i> , (c) <i>DSC</i> and (d) <i>DTC-CSF2</i>	119
5.20	Comparison by experimentation of torque capability in flux weakening region obtained in (a) <i>DTC-HYS1</i> , (b) <i>DTC-HYS3</i> and (c) <i>DTC-CSF2</i> (Time scale: 400ms/div.)	120
5.21	Comparison of torque dynamic performance in a flux weakening region, obtained in (a) <i>DTC-HYS1</i> , (b) <i>DTC-HYS3</i> and (c) <i>DTC-CSF2</i> (which is corresponded to the results obtained in Figure 5.20) (Time scale: 40ms/div.)	121
6.1	Complete drive system (a) picture of the experiment set-up, (b) functional block diagram of the experiment set-up	123
6.2	Identifying sectors of the stator flux (a) definition of $\Psi_{sq,1}$, (b) determining sector based on threshold values, i.e. 0 and $\Psi_{sq,1}$	125
6.3	Identifying sectors of the stator flux (a) definition of $\Psi_{sq,1}$, (b) determining sector using $\Psi_{sq,1}$	127
6.4	Altera FPGA (APEX20KE)	129
6.5	Block diagram of voltage vectors selection table and blanking time generation	131
6.6	Block diagram of blanking time generation for a single leg (i.e. phase <i>a</i>)	131

6.7	Timing diagram of blanking time generation for a single leg (i.e. phase <i>a</i>)	132
6.8	Schematic of the gate driver circuit	133
6.9	Schematic of the IGBT module with the capacitor Snubbers	134
6.10	Gate drivers and VSI	134
6.11	A coupling between induction machine (right) and DC machine (left)	136

LIST OF SYMBOLS AND ABBREVIATIONS

AC	-	Alternating Current
ADC	-	Analog to digital converter
B	-	Viscous friction
CFTC	-	Constant Frequency Torque Controller
C_{upper}	-	Upper triangular carrier
C_{lower}	-	Lower triangular carrier
C_{p-p}	-	Peak to peak value of the triangular carrier
d,q	-	Direct and quadrature axis of the stationary reference frame
d^{Ψ_s}, q^{Ψ_s}	-	Direct and quadrature axis of the estimated stator flux reference frame
DAC	-	Digital to analog converter
DC	-	Direct Current
DSP	-	Digital Signal Processor
DTC	-	Direct Torque Control
DSC	-	Direct Self Control
emf	-	Electromotive force
f_c	-	Carrier frequency
f_{sw}	-	Switching frequency
FOC	-	Field Oriented Control
FPGA	-	Field Programmable Gate Array
I.E	-	Incremental Encoder
I.M	-	Induction Machine
i_s^g, i_r^g	-	Stator and rotor current space vectors in general reference frame
i_s, i_r	-	Stator and rotor current space vectors in stationary reference frame
i_{rd}, i_{rq}	-	d and q components of the rotor current in stationary

	-	reference frame
i_{sd}, i_{sq}	-	d and q components of the stator current in stationary reference frame
J	-	Moment of inertia
k_p	-	Proportional gain of the PI controller for CFTC
k_{pw}	-	Proportional gain of the PI controller for speed controller
k_i	-	Integral gain of the PI controller for CFTC
k_{pw}	-	Integral gain of the PI controller for speed controller
L_m	-	Mutual inductance
L_s	-	Stator self-inductance
L_r	-	Rotor self-inductance
P	-	Number of pole pairs
PI	-	Proportional - Integral
p.p.r	-	Pulse per revolution
PWM	-	Pulse Width Modulation
R_s, R_r	-	Stator and rotor resistance
r.m.s	-	Root mean squared
SVM	-	Space Vector Modulation
S_a, S_b, S_c	-	Switching states of phase a, b, c
T_e	-	Electromagnetic torque
$T_{e, rated}$	-	Torque rated
$T_{e, ref}$	-	Reference torque
T_{PI}	-	Output of PI controller for the CFTC
T_{stat}	-	Torque error status
t_{tri}	-	Period of C_{upper} or C_{lower}
THD	-	Total Harmonic Distortion
V_{DC}	-	DC link voltage
v_s^g	-	Stator voltage space vector in general reference frame
v_s	-	Stator voltage space vector in stationary reference frame
v_{sd}, v_{sq}	-	d and q components of the stator voltage in stationary reference frame
VHDL	-	VHSIC hardware description language
VSI	-	Voltage Source Inverter
α_h	-	Angle within sector h

θ_r	-	Angle with respect to rotor axis
θ_s	-	Angle with respect to stator axis
δ_{sr}	-	Difference angle between stator flux linkage and rotor flux linkage
Ψ_s^g, Ψ_r^g	-	Stator and rotor flux linkage space vectors in general reference frame
Ψ_s, Ψ_r	-	Stator and rotor flux linkage space vectors in stationary reference frame
Ψ_s	-	Estimated stator flux linkage
Ψ_{sd}, Ψ_{sq}	-	d and q components of stator flux in stationary reference frame
$\Psi_{sd}^{\Psi_s}, \Psi_{sq}^{\Psi_s}$	-	d and q components of stator flux in stator flux reference frame
ω_r	-	Rotor electrical speed in rad./s
ω_e	-	Steady state synchronous frequency in rad./s
ω_m	-	Rotor mechanical speed in rad./s
ω_{slip}	-	Steady state slip frequency in rad./s
σ	-	Total flux leakage factor
τ_r	-	Rotor time constant

LIST OF APPENDICES

APPENDIX	TITLE	PAGE
A	Derivation of torque and flux equations	151
B	Derivation of torque rate equation	153
C	Derivation of the relationship between the angle δ_{sr} and the slip angular frequency	156
D	Simulation of DTC	158
E	DSP source code listings	164
F	VHDL code	178
G	List of Publications	184

CHAPTER 1

INTRODUCTION

1.1 A Look Back on Development of Vector Control Induction Machine Drives

In the past decades, DC machines have been used extensively in many applications due to its simplicity and offers high performance torque control. Their mechanical commutation action forms the torque and flux components that are always orthogonal, which allows high performance control achieved under optimal conditions. Despite their excellent performance and simple control structure, the construction using the mechanical commutator and brush cause some limitations. For examples, they require regular maintenance and cannot be operated in the dirty or explosive environment, their speed is limited and they are expensive. Unlike DC machines, the induction machines are robust, require less maintenance, cheaper and able to operate at higher speed. The induction machines became popular and gradually replacing DC machine drives in many industrial applications as the Field Oriented Control (FOC) introduced by F. Blachke in 1970's can produce comparable performance to that obtained in DC machines [1]. Moreover, their popularity is also assisted by the rapid development in power semiconductor devices and the emergence of high-speed microprocessor and digital signal processors [2]. FOC of induction machines can provide a decoupled control of torque and flux using their respective producing current components, which is similar to the DC machine control method. This is possible by considering the stator current vector in the rotating reference frame so that the orthogonal components of the stator current (represent as torque and flux producing current components) appear as DC

quantities. The rotating reference frame refers to the rotating space vector quantity which can be either rotor flux or stator flux. The one which is based on rotor flux (referred as Rotor Flux Oriented Control (RFOC)) is sensitive to the parameter variations, and also it requires the knowledge of rotor speed. The improvements of the FOC performance were reported in many technical papers; these include the areas of robust control [3-5], improved flux estimator [6-9] and sensorless speed control [10-12].

1.2 Direct Torque Control of Induction Machines

Over the past years, Direct Torque Control (DTC) scheme for induction motor drives [13] has received enormous attention in industrial motor drive applications. It was also used as the main platform for the ABB inverter technology, and the first DTC drive was marketed by ABB in 1996 [14-15]. Its popularity increases since it offers a faster instantaneous dynamic control and its control structure is simpler compared to the field-oriented control (FOC) scheme [13, 16-17]. In DTC, the torque and flux are controlled independently, in which their demands are satisfied simultaneously using optimum voltage vectors. Unlike the FOC drives, where the torque and flux are controlled corresponded to their producing current components (i.e. d and q axis components of stator current) which requires frame transformer, knowledge of machine parameters and current regulated Pulse Width Modulation (PWM).

1.2.1 The Structure of Basic DTC

The simple control structure of DTC proposed by Takahashi [13] is shown in Figure 1.1. It contains a pair of hysteresis comparators, torque and flux estimators, switching table for voltage vectors selection and a 3-phase Voltage Source Inverter (VSI). A decoupled control structure is provided in the scheme, wherein the electromagnetic torque and the stator flux can be controlled independently using 3-

level and 2-level hysteresis comparators, respectively. To satisfy the torque and flux demands, the appropriate voltage vector for a particular flux sector should be chosen, either to increase torque or to reduce torque and at the same time either to increase stator flux or to decrease stator flux; based on torque error status, flux error status and flux orientation. In fact, high performance control in DTC drive with proper selection of voltage vectors can be established if the flux as well as torque is estimated accurately. A combination of the voltage model and the current model using a first-order lag network was implemented in [13] to obtain a proper flux estimator for entire speed range operations. The use of the current model is superior in estimating the flux at very low speed operations, but it requires the knowledge of motor speed, which in turns requires an observer or a speed sensor from the motor shaft. On the other hand, the implementation of the voltage model provides better flux estimation for high speed operations and requires only stator resistance and terminal quantities (i.e. stator voltages and stator currents), which leads to the robust control of DTC. However, the digital implementation of this model utilizing microprocessor or digital signal processor introduces some problems, i.e. the integration drift and initial condition problems [18-20].

In hysteresis-based DTC, the switching frequency of VSI is totally contributed by the switching in the hysteresis comparators. It was highlighted in [21-23] that the slopes of torque and flux, which relatively affect the switching in their hysteresis comparators, vary with the operating conditions (i.e. rotor speed, stator and rotor fluxes and DC link voltage). This causes the switching frequency of VSI also varies with the operating conditions. The variation in the switching frequency as a result produces unpredictable harmonic current flow. For this reason, the switching devices cannot be fully utilized to its maximum frequency capability for most operating conditions, since the selection of hysteresis band's width is based on the worst condition.

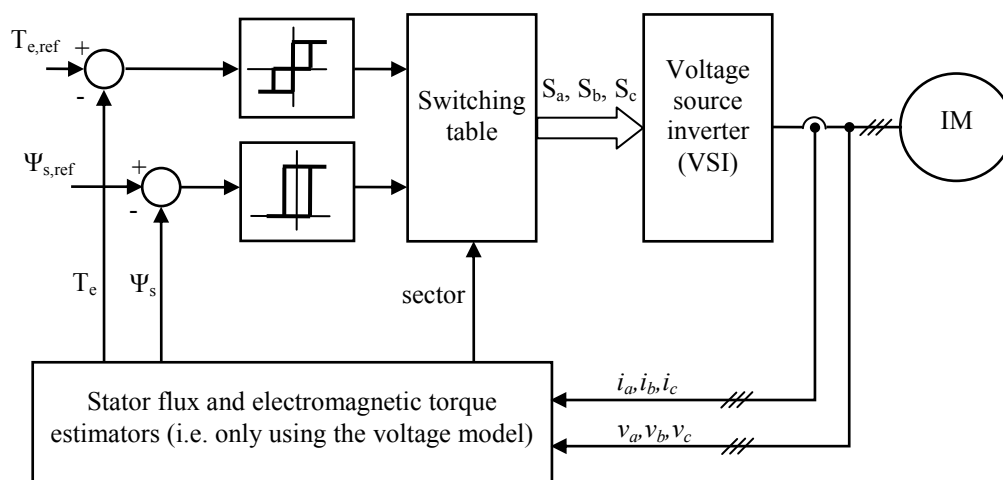


Figure 1.1 Control structure of basic DTC-hysteresis based induction machine

1.2.2 Improvements of DTC Performance

Since DTC was first introduced in 1986 [13], several variations to its original structure (which referred to as DTC hysteresis-based) were proposed to improve the performance of DTC of induction machines. Noticeably, most researches in last decades aimed to overcome the inherent disadvantages of hysteresis-based DTC schemes, such as variable switching frequency and high torque ripple. In addition, some recent researches interested to facilitate the DTC to be operated in overmodulation mode that will improve the dynamic performance and the power output of DTC of induction machines. To relate the study of this thesis, some reviews on improvements of DTC are concentrated into three following research areas:

- *Torque Ripple Reduction or/and Constant Switching Frequency*

Basically, the output torque ripple can be reduced by reducing the band width of hysteresis comparator to the appropriate value. The selection of the appropriate

band width is based on the worst operating conditions [24]. This will ensure the switching frequency of switching devices do not exceed its limit (or thermal restriction). It is also desirable to use a high speed processor to keep the ripple within the band, in such a way the discrete hysteresis controller will perform like the analog one.

Instead of decreasing the hysteresis band and using a high speed processor, the ripple can be minimized by injecting high-frequency triangular waveforms to the errors of torque and flux [25]. This method is called dithering technique, which is simple and effective to minimize the torque ripple even performing DTC at limited sampling frequency. However, it still produces unpredictable switching frequency since the torque and flux slopes which are related to the switching frequency, do vary with operating conditions [23, 26].

Several methods had been proposed to provide a constant switching frequency as well as reduced output torque ripple [22, 27-38]. In [27], a constant switching frequency is established in the hysteresis-based DTC by adjusting the band width of the hysteresis comparators according to the changes in operating conditions. The adjustable of band width is based on a PI controller and a pulse counter, for each comparator. This, consequently, increases the complexity of the DTC drive. Moreover, this technique does not guarantee reduction of torque ripple as it is inevitable in the implementation of discrete hysteresis controllers. Another approach to minimize the torque ripple is to control the DTC switching based on optimal switching instant that satisfies the minimum-torque ripple condition [22, 29-30]. In this way, the term so called a duty ratio is determined so that the appropriate active state is switched for some portion of a switching period, and the zero vector is selected for the rest of the period. It was shown in [24] that the switching frequency is strongly affected by the torque hysteresis band. Thus, it makes sense that the almost constant switching frequency as well as reduced torque ripple can be achieved if the control of torque error is performed at a higher and a constant frequency. As proposed by [32], the principal operation of torque controller using the hysteresis-based is replaced with a triangular carrier-based. The improvement is achieved and at the same time retains the simple control structure of DTC. The most common

approach to solve the problems is using the space vector modulation [28, 31, 33-35]. In this approach, the switching period is subdivided into three or more states, to synthesize the desired voltage vector in order to produce the minimum torque ripple.

Recently, predictive control strategy to DTC has gain considerable amount of attention particularly due to its ability to reduce the torque ripple and switching frequency [36-39]. In particular model predictive control (MPC) which was applied in [38] and [36] uses the hysteresis comparators but with the switching table replaced with online optimization algorithm.

- *Fast Torque Dynamic Control through Dynamic Overmodulation Strategy*

Without the need to use any extra hardware, the torque dynamic performance can be improved by fully utilizing the available DC link voltage through overmodulation. To perform the DTC under the overmodulation mode, it is preferable to use the Space Vector Modulation (SVM) [28, 40-44] rather than other techniques (for example, [45-46] use the triangular carrier based). This is because, the SVM is more flexible to be adopted for advanced motor control where only a single reference voltage vector $\mathbf{v}_{s,ref}$ is employed to define the mode of overmodulation.

During large torque demand, it is inevitable that the reference voltage $\mathbf{v}_{s,ref}$ exceeds the voltage vector limits enclosed by the hexagonal boundary. Under this condition, the SVM has to be operated in what is termed as dynamic overmodulation mode. The voltage reference vector $\mathbf{v}_{s,ref}$ has to be modified such that it will lie on the hexagonal boundary.

Several methods [28, 43, 47-49] have been proposed and to some extent, these methods have managed to minimize the voltage vector error as well as obtained a fast torque response. Figure 1.2 compares some modified voltage references, $\mathbf{v}_{[i]}$ (e.g. when $i = 1$, proposed in [1]) with respect to the original voltage reference vector,

$v_{s,ref}$, which is beyond the hexagonal boundary of the voltage vectors. Note that, voltage vector components are not drawn to scale. It can be seen that (from Figure 1.2), [42] and [50] switched only single voltage vector which is $v_{s,h+2}$ during dynamic overmodulation. This single selection of vector shows the occurrence of a six-step operation that produces the fastest dynamic torque control as will be discussed later in Chapter 4. While the other methods result in slower dynamic torque response since two active states are alternately switched during the dynamic condition. For example, [28] used two active states utilizing dead-beat control in order to maintain the magnitude of stator flux under control for any condition. Later, [43] was proposed to simplify the complexity control structure in [28], (where it does not provide a dead beat control of the magnitude flux as a transient torque encountered) and hence results in a faster dynamic torque control. In this way, the modified voltage vector, $v_{[43]}$ has the same angle, γ as the original reference voltage, $v_{s,ref}$ but with a modified magnitude. In [47], the reference voltage, $v_{s,ref}$ was modified to $v_{[47]}$ such that the error between the magnitude of $v_{[47]}$ and $v_{s,ref}$ is minimized. This means the modified voltage vector, $v_{[47]}$ should be closest to the original reference vector $v_{s,ref}$ by ensuring that a line joining the $v_{s,ref}$ and $v_{[47]}$ is orthogonal to the hexagon boundary.

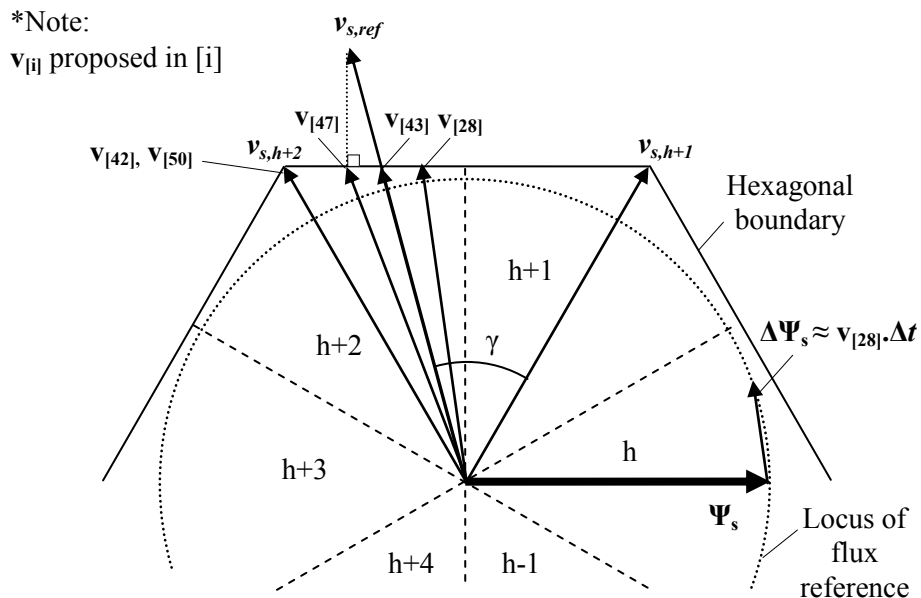


Figure 1.2 Variations of modified reference voltage vectors which is applied during dynamic overmodulation mode

- *Enhanced Torque Capability using Flux Weakening or/and Overmodulation Strategy*

A wide-speed high torque capability is a very important feature in many electric motor drive applications. In automotive applications, it is usually referred to as a high 'Constant Power Speed Range' (CPSR). The availability of wide range of speed operations with the maximum capability of torque is of main concern, especially for the road electric vehicles where multiple gears have to be avoided.

In practice, a flux weakening strategy is normally used to extend the motor speed operations beyond the base speed and to enhance the capability of torque. Several papers were published [42, 50-63] proposing the solution of achieving maximum torque capability in field weakening region. The common approach adopted is to estimate the optimal flux level of the motor based on the maximum values of inverter voltage and inverter current. Typically, the algorithms require frame transformer, knowledge of machine parameters and space-vector modulator. For examples, [53] used Field Oriented Control-Space Vector Modulation (FOC-SVM) while [63] used Direct Torque Control-Space Vector Modulation (DTC-SVM), and they consider voltage and current limit conditions to compute the controllable currents (in stator flux reference frame) in achieving the appropriate flux level in field weakening region. Besides that, some papers had been reported to provide a robust field weakening strategy so that any variations of machine parameters used in calculating the optimal flux can be compensated [55, 59, 61-62].

In order to achieve the fastest torque dynamic response as well as high torque capability in a flux weakening region, the DTC needs to have the capability to operate in six-step mode. However, only a few schemes have the ability to perform this; i.e. [42] used DTC-SVM with the predictive-deadbeat control and [50] used Direct Self Control with hexagonal flux operation.

1.2.3 The Popularity Versus The Complexity of DTC-SVM based induction machines

The most popular variation of DTC of induction motor drives is the one that is based on space vector modulation (SVM), which normally referred to as DTC-SVM [28, 33, 40, 42, 64-66]. As mentioned previously, the advantages provided by this scheme not only solve the inherent problems in hysteresis-based DTC but also facilitate the DTC performs under overmodulation region. Moreover, the study of the SVM itself in the area of overmodulation strategy improvement for 3-phase VSI was reported by many researchers [41, 46-47, 49, 66-73]. All these evidences show that the implementation of SVM to operate under overmodulation region is well established, and widely adopted for advanced motor control.

The major difference between DTC hysteresis-based and DTC-SVM is the way the stator voltage is generated. In DTC hysteresis-based the applied stator voltage depends on voltage vectors, which are selected from a look-up table. The selections are based on the requirement of the torque and flux demand obtained from the hysteresis comparators. On the other hand, in DTC-SVM, a stator voltage reference is calculated or generated within a sampling period, which is then synthesized using the space vector modulator. The stator voltage reference vector is calculated based on the requirement of torque and flux demands. Due to the regular sampling in SVM, the DTC-SVM produces constant switching frequency as opposed to the variable switching frequency in hysteresis-based DTC however, at the expense of more complex implementation.

The generation of reference voltage $v_{s,ref}$ often involves complex calculation. For examples; [28] used dead-beat control with several complicated equations (i.e. quadratic equations) to generate the reference voltage in real-time and [64] utilized predictive control of stator flux error vector to estimate the reference voltage and needed extra calculation on the synchronous angular velocity. While the others include the use of proportional-integral current controller [40], stator flux vector error [65, 74-75], proportional-integral torque and flux controllers [33, 76-77], predictive and dead-beat controllers [42-43]. Moreover, the implementation of DTC-

SVM becomes complicated as the reference voltage needs to modify whenever it passes outside the hexagon (due to the physical constraint of inverter as the $v_{s,ref}$ defines mode of overmodulation), particularly during a large torque demand. Some modified reference voltages as mentioned previously are shown in Figure 1.2.

Figure 1.3 shows a general block diagram of generation of switching in DTC-SVM, which contains three main components and the functional of the two of them are as mentioned above.

Ultimately, all of the proposed methods [28, 33, 40, 42-43, 64-65, 74-77] complicate the basic control structure of DTC drive systems as originally proposed in [13].

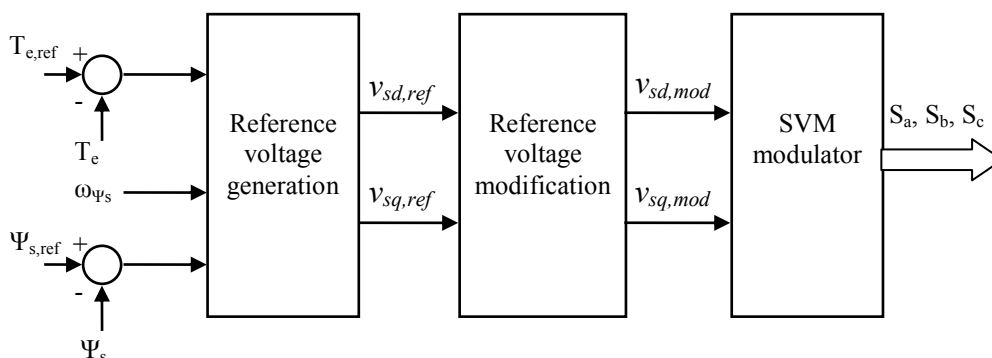


Figure 1.3 A general block diagram of generation of switching in DTC-SVM

1.3 Thesis Objectives and Contributions

The objective of this thesis is to study, implement and improve the performance of the DTC of induction machines. Despite the improvements, the proposed methods also aim to preserve the simple control structure of DTC drive. The thesis proposes a simple, yet significant, method of overmodulation strategy employed in the DTC-hysteresis based induction machine to improve torque dynamic control and to enhance torque capability for a wide speed range operation.

The thesis also shows that the proposed methods can be implemented using a constant switching controller [32] (which has a similar control structure with the hysteresis-based DTC), in order to give extra advantages of providing a constant switching frequency and reduced torque ripple. While doing the research, the thesis makes the following contributions:

- It shows the reduction of torque ripple in [32] can be further reduced by enlarging the constant frequency of triangular carriers. This is achieved without the need of reducing the sampling period which is useful for the DSP or microprocessor with a limited sampling frequency.
- It analyses the effect of different voltage vectors selection on the performance of torque dynamic control in DTC induction machine drive. Although the hysteresis-based DTC is well established to give a high performance torque control, there is still room to further improve the performance based on the observation of the analysis.
- It introduces a modification block of flux error status in the hysteresis-based DTC drive which is responsible to perform dynamic overmodulation. This technique is very simple, yet it gives the fastest torque dynamic control. The introduced block can also be implemented in [32] to verify the improvements.
- It justifies the extension of constant torque region and hence improvement of torque capability can be obtained by controlling the locus of flux into hexagonal shape. With this method, the stator voltage in the DTC drives (i.e. in [32] and hysteresis-based DTC) can be transformed with a smooth transition from PWM to the six-step mode.
- It describes the modification of flux error status to establish the control of hexagonal flux locus, particularly during dynamic conditions (i.e. large torque demand or motor acceleration). The hybrid DTC is proposed to operate the control of flux into dual mode, i.e. circular flux locus as

performed in DTC during the steady state (that produces lower current's THD) and hexagonal flux locus as performed in Direct Self Control (DSC) when dynamic condition encountered (that gives superior dynamic performance). The feasibility of the proposed method is verified using the hysteresis-based DTC and the scheme proposed by [32].

- It improves dynamic performances in flux weakening region. With the proposed overmodulation strategy, the fastest torque dynamic control and higher torque capability are achieved with the complete six-step voltage.
- It introduces a step reduction of reference flux to ensure proper torque control when a motor speed reaches its target in a flux weakening region. This is to avoid an inappropriate level of reference flux (i.e. too high flux level) as the hexagonal flux changes to the circular.
- It develops a simulation and experimental set-up to verify the proposed improvements on the DTC drive. The simulation is based on Matlab and Simulink program from Mathworks inc.. The experimental set-up consists of a DS1102 DSP controller board as the main processor and APEX20KE Altera FPGA. The combined controller board is implemented so that the sampling period of the DSP can be minimized by distributing some of the tasks to the FPGA.

1.4 Methodology of Research

A novelty of the overmodulation strategy was developed by investigating various overmodulation strategies, particularly associated with the SVM approach. The switching pattern of the voltage vectors in overmodulation region was translated or mapped onto the stator flux plane since there is no reference voltage vector in the hysteresis-based DTC. A thorough investigation on the various flux weakening

strategies, constant switching frequency and reduced torque ripple strategy was also carried out.

The development of the overmodulation strategy for the hysteresis-based DTC is based on the modification of flux error status on the stator flux plane. To achieve the fastest torque dynamic control, the most optimized voltage vector is switched and held. The selection of the voltage is determined by the modified flux error status. To enhance torque capability, the proposed overmodulation and flux weakening strategies are utilized in the hybrid DTC scheme. This scheme performs the control of flux in dual mode operations. This is established using the introduced block named as 'block of Modification of Flux Error Status'. The improvements using the proposed methods also can be achieved with the extra advantages, i.e. reduced torque ripple and constant switching frequency using the scheme proposed by [32].

Once the algorithm for the overmodulation and field weakening was developed, it had to be applied to the DTC drive and simulated using large signal model. The Matlab/SIMULINK simulation package was used for this purpose.

The proposed overmodulation and field weakening strategies utilizing a hybrid DTC scheme had been verified and evaluated for its feasibility and effectiveness through hardware implementation. A state-of-the-art digital signal processor and field programmable gate array devices (DS1102 controller board and APEX20KE Altera FPGA) were used to implement the DTC controllers including the overmodulation and field weakening strategies. A standard induction machine with suitable loads and IGBT-based VSI had been used for this purpose.

1.5 Organisation of the Thesis

The rest of the thesis is organised as follows:

Chapter 2 describes the mathematical modeling of induction machine and the basic principle of DTC of induction machines. The inherent problems in discrete implementation of hysteresis-based DTC such as variable switching frequency, high torque ripple and the need of high speed processor are also discussed.

Chapter 3 suggests to use the simple method proposed by [32] to perform a constant switching frequency and to reduce output torque ripple, instead of using the common approach that is SVM. A quick guide to design or to obtain a proper controller of the Constant Frequency Torque Controller (CFTC) is presented. Further improvement in reducing the torque ripple can be achieved by extending the triangular carrier frequency to its maximum (which is equal to one-quarter of the maximum sampling frequency achieved by the DSP).

Chapter 4 proposes a simple dynamic overmodulation to achieve the fastest torque dynamic control. The effect of selecting two possible voltage vectors on the torque dynamic performance is analyzed. Based on the observation, the most optimized voltage vector is identified, and it is used to produce the fastest torque dynamic response. Simulation and experimental results are presented to show the effectiveness of the proposed method. Experimental results on the proposed method implemented in [32] is also presented.

Chapter 5 proposes a simple overmodulation and flux weakening strategy utilizing hybrid DTC scheme. The hybrid DTC scheme is constructed to facilitate the DTC drive to operate similar to that of DSC, which is based on hexagonal flux locus. By controlling the locus flux into hexagonal shape, the limit of stator voltage can be reached up to the six-step mode as the motor operates in flux weakening region. As a result, the hybrid DTC performs at higher torque capability and hence gives a lesser motor acceleration time. Simulation and experimentation as well as comparison with

the conventional DTC scheme to verify the feasibility of the proposed method, are presented. Experimental results on the proposed method implemented in [32] is also presented.

Chapter 6 describes the experimental set-up used in the thesis. Details information of each hardware component and the implementation of the tasks are given.

Chapter 7 gives the conclusion of the thesis and possible directions of further research.